On the usability of polymer-based artificial tendons for elastic energy storage in active ankle prostheses

Jeanne Evrard[1], François Heremans[1] and Renaud Ronsse[1]

***Abstract*— In the recent past, the development of lower-limb prostheses has taken a new turn with the emergence of active systems. However, their intrinsic wearable nature induces strict requirements regarding weight and encumbrance. In order to reduce the load — and thus the bulkiness — of their active part, several prototypes leverage the concept of compliant actuation, consisting in including an elastic element in parallel and/or in series with the actuator. In this paper, we explore the usability of polymer compliant ropes placed in parallel with the actuator of an ankle prosthesis. Ropes are intrinsically light and compact, and thus offer several advantages as compared to more traditional coil or leaf springs. Polymer materials were selected for their high energy density and yield strength. We conducted a set of experimental tests with several ropes, pretension levels, and periodic loading profiles. Results show that polymer-based ropes have a high potential for ankle assistance devices, since they can store the required energy in a low volume. However, further research should be conducted to improve their efficiency, since we estimated that only about $50\,\%$ of the stored energy can be released, with few variations as a function of the rope preconditioning and loading profile.**

I. INTRODUCTION

Nowadays in Europe, the number of major lower limb amputations is approximately 20 per 100,000 inhabitants per year [1]. After lower limb amputation, a patient can be fitted with a prosthesis to replace the missing limb and thus to restore locomotion. The vast majority of ankle prostheses on the market nowadays are passive [3]. During the stance phase of walking, the most advanced models store elastic energy in a compliant element and return it later during the push-off phase. Energy Storing And Return (ESAR) feet do not provide net positive energy as biological ankle muscles do during walking [4]. Moreover, they are not able to adapt this energy profile to the environment, such as slopes or stairs [5]. Unilateral lower-limb amputees tend to have an asymmetric gait due to this lack of propulsion during push-off [6], [7]. This induces comorbidities such as back pain and osteoarthritis due to a compensatory loading of the intact leg. These injuries are more likely to occur if the prosthesis has been worn for a long time [8], [9].

Consequently, recent development of active ankle prostheses was driven by the need of providing net energy to the amputee's prosthetic joint [10], although it remains unclear whether it will prevent overuse of the intact joints [11]. Designing an ankle prosthesis is challenged by strict requirements regarding volume, weight, noise, power and energetic autonomy. The first active device was designed by MIT (USA) and dates back to 2006. This prosthesis is powered by a Series Elastic Actuator (SEA) and a carbon composite leaf spring structure is used to store elastic energy [12]. This prototype and its successive developments led to the first commercialized powered prosthesis called the EmPower, by Ottobock (Duderstadt, Germany). Other prosthetic ankles with compliant actuators are under active development, such as the TF8 [13] and the Utah Bionic Leg [14].

All these devices have elastic elements included in the actuation chain, placed in parallel (Parallel Elastic Actuator, PEA) and/or in series (SEA) with the actuator. Both configurations have the potential to improve energy efficiency [15]. SEA can indeed decrease the velocity peak that the actuator should follow to deliver the required energy, while PEA can flatten the actuator torque profile by storing elastic energy in parallel to the actuation chain. Both have thus a direct impact in reducing fluctuations of the power profile [16], [17]. The selected actuator can then be smaller, lighter, safer, and cheaper.

In the devices mentioned above, carbon leaves or steel springs are used as elastic elements. As benchmarks, these spring assemblies weight about $120\,g$ in both Utah [14] and TF8 [13] foot prostheses. In this paper, we explore the usability of a concurrent technology for elastic energy storage, i.e. polymer-based ropes. Elastic ropes have indeed the advantage of being light – a few grams only – and compact. More specifically, we aim at characterizing the elastic elements of the Efficient Lockable Parallel Spring Ankle (ELSA) prosthesis [18]. In its original design, we used polyamide ropes to implement a Lockable Parallel Spring. It was directly inspired by the plantar fashia and Archilles tendon of the biological ankle. Pilot experiments conducted with this prototype raised some concerns about the efficiency of these ropes, as visualized by hystheresis in their force vs. position relationship. The aim of the present paper is to investigate this efficiency more systematically. Furthermore, we investigated whether other polymer-based ropes have better specifications for an ankle prosthesis application. Due to space constraints in a prosthetic foot, such ropes have to withstand large deformations relatively to their active length. In practice, two materials were selected given their high energy density and yield strength, i.e. polyamide and polyester.

The rest of the paper is structured as follows. Section II states the problem, i.e. details the requirements of a rope-like elastic element used in the actuation chain of an ankle prosthesis application. Experimental methods are then detailed in Section III. Results are described and discussed

[1]Institute of Mechanics, Materials, and Civil Engineering (iMMC) and Louvain Bionics, Université catholique de Louvain, Belgium jeanne.evrard@uclouvain.be

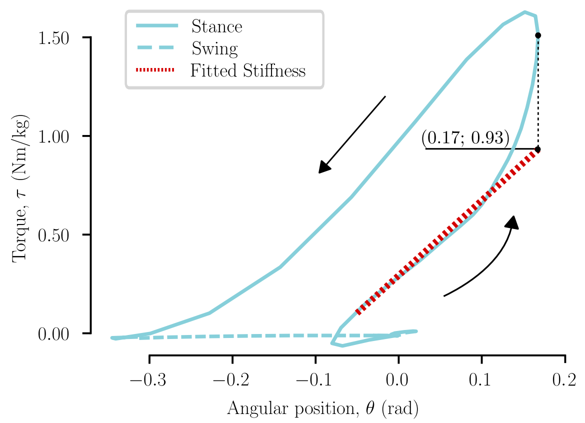

Fig. 1. Torque vs. angular ankle trajectory in normal walking, data adapted from [19]. In our given application of ankle prosthesis, the contribution from an ideal passive elastic element is highlighted by the equivalent stiffness fitting the first part of the stance phase (dotted red curve).

in Section IV, followed by the last section concluding the paper.

II. PROBLEM STATEMENT

In this section, we establish the mechanical requirements being specific to polymer-based artificial tendons that would be used in an ankle prosthesis. These requirements are quantified from previously published kinematic and kinetic trajectories of the ankle [19], as depicted in Fig. 1. This graph highlights that a sound ankle provides mechanical work during walking, since the curve follows a counter-clockwise pattern over the cycle. Therefore, an active system is necessary if we want to reproduce this behavior with a prosthesis. Furthermore, it shows that a passive elastic element placed in parallel to the actuator can also capture a significant fraction of this curve. In particular, it should be triggered at the beginning of the stance phase and stay active during all this phase, i.e. when torque has to be produced. In sum, active and passive elements should be combined in a way that the passive element mitigates the torque to be provided by the active element.

Optimization from [20] revealed that an ideal passive element acting in parallel to the actuator of an ankle assistive device should: (i) have a stiffness close to the linear interpolation of the rising edge of the torque-position curve during the stance phase; and (ii) be active only above a certain angular threshold θ_A, corresponding to the beginning of the stance phase. This is indeed what would result in the most appropriate level of energy storage. At maximal dorsiflexion angle, i.e. $0.17\,rad$, the passive element should then provide a torque of $0.93\,Nm/kg$ or $69.75\,Nm$ for a $75\,kg$ user, i.e. the median weight of an adult population. This torque is noted τ_{EB} and represents the passive torque delivered by the elastic element to the user's body. It corresponds to about $57\,\%$ of the target total ankle torque.

Fig. 2 shows the schematic representation of an ankle prosthesis, with the angle between the lever arm and the vertical axis noted θ. As this angle increases, the elastic element becomes tighter. The unidirectional rigid connection between the joint and the elastic element has a length d

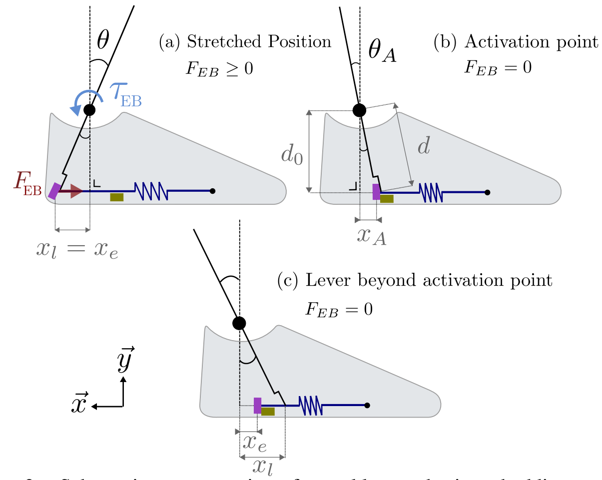

Fig. 2. Schematic representation of an ankle prosthesis embedding a rope-like parallel elastic element. θ denotes the ankle angle, x_l and x_e are the horizontal displacements between the position corresponding to $\theta = 0$ and, the end of the lever and the end of the elastic element, respectively. τ_{EB} is the passive torque that should be delivered at the joint level by the elastic element to the user's body. (a) When the lever pulls the elastic element though the purple interface, the elastic force F_{EB} is positive and generates some ankle torque. (b) When $\theta = \theta_A$, the elastic element is blocked by a mechanical stop (green). (c) The lever can freely move further in plantarflexion, while the elastic element is hold by the mechanical stop.

that varies according to the angle θ. When the joint is perpendicular to the elastic element, $\theta = 0\,rad$ and $d = d_0$.

The design specifications should be provided in a frame attached to the elastic element. Therefore, typical ankle torque and angle profiles should be converted into a prismatic frame, i.e. into force F_{EB} and linear position of the lever x_l. These geometrical relationships are obtained from Fig. 2:

$$F_{EB} = \frac{\tau_{EB}}{d_0}, \qquad (kN) \tag{1}$$

$$x_l = d_0 \tan(\theta), \qquad (mm) \tag{2}$$

The position of the end of the elastic element is noted x_e. The position $x_A = d_0 \tan \theta_A$ corresponds to the fixed position where the elastic element starts to be engaged by the lever. The positions of the elastic element, i.e. x_e, and of the lever, i.e. x_l, are equal when x_l is larger than the activation position x_A. Indeed, when the lever exceeds this limit in plantarflexion, the elastic element is blocked by a mechanical stop, and the lever continues its movement freely.

$$x_e = \begin{cases} x_l, & \text{if } x_l > x_A \\ x_A, & \text{otherwise} \end{cases} \tag{3}$$

From the equations above, the linear stiffness k_x of the rope can be computed, assuming that no force is produced at x_A:

$$k_x = \frac{F_{EB}}{x_e - x_A}, \qquad (kN/mm) \tag{4}$$

From the passive torque identified previously, the maximal linear force is thus equal to $F_{EB} = 1.48\,kN$, from Eq. (1), when $x_e = 8\,mm$, from Eq. (2). The corresponding target stiffness k_x is thus equal to $0.15\,kN/mm$. These specifications were obtained by taking $d_0 = 47\,mm$ and $x_A = -2\,mm$, in compliance with the available volume of

a typical prosthetic foot.
As points of comparison, [21] studied a variable stiffness foot having a stiffness of about $9\,Nm/deg$ during dorsiflexion for a $100\,kg$ user, which can be converted to $5.2\,Nm/rad/kg$. This is in the same range of our calculated stiffness which is equal to $4.4\,Nm/rad/kg$.

The elastic element covers a range of motion going from the activation angle, i.e. $\theta_A = -0.04\,rad$, to the maximum dorsiflexion angle. This corresponds thus to an angular range of $0.21\,rad$, i.e. a linear elongation of $10\,mm$, see Eq. (2). Due to volume constraints within a typical prosthetic foot, the resting length of the elastic element should be about $80\,mm$. The corresponding deformation is thus about $13\,\%$.

In sum, the ideal elastic tendon for our ankle assistive device, considering a mid-range user of $75\,kg$, should have the following features :

- The capacity to withstand stretching forces up to $1.48\,kN$ in the elastic regime.
- A total equivalent linear stiffness of about $0.15\,kN/mm$.
- A strain of about $13\,\%$ in the elastic regime.
- An energy efficiency as high as possible in order to minimize active energy to be provided by the actuator, since the elastic element is placed in parallel to it.

III. Methods

In the present section, we introduce polyester and polyamide as two candidates for our ankle prosthesis application. Then, a brief description of the mechanical setup is exposed, followed by the experimental methods. Finally, we address the calculation of the stiffness and energy losses.

A. Material Selection

In order to meet the specifications identified in Section II, the choice was made to place the rope in a closed loop – running back and forth – in our implementation. The total length of the rope at rest is then equal to twice the identified characteristic length, i.e. $160\,mm$. By placing two rope segments in parallel, the force withstood by each part is equal to $0.76\,kN$, i.e $0.5\,F_{EB}$.

A good energy storing material should have a high breaking strength, a large elongation at break and negligible creep at the same time. Polyester (PE) and polyamide (PA) fibers were selected for our application. Material such as Aramide was excluded because of its too low elongation. Although Polypropylene has good characteristics, it has a tendency to creep at high loads [23]. Three ropes with a diameter of $3\,mm$ with different strand configurations were selected, to fit within the typical available volume in such a device. The characteristics of these three ropes – PA1, PA2 and PE – are listed in Table I.

Breaking strength of each rope is about $1.5\,kN$ (Table I), providing a safety factor of two. The three ropes can deform up to more than 15% without breaking, which is again larger than the threshold we identified. However, the elongation at break does not provide information about the region where the material takes plastic deformations. One of the objectives of the experimental trials will be to assess if the ropes stay in their elastic regime for deformations up to $13\,\%$, while their elongation at break is reported to be between $15\,\%$ and $20\,\%$ (for PE) and between $16\,\%$ and $27\,\%$ (for PA).

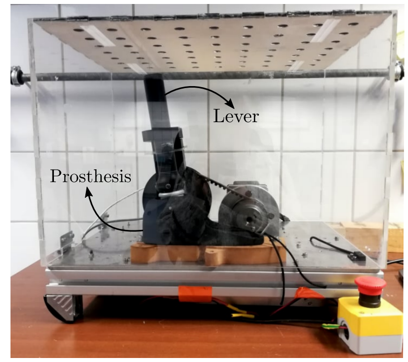

Fig. 3. Experimental setup: the tested rope is embedded into a simplified prosthetic foot, in a configuration similar to the one pictured in Fig. 2. A motor is used to move the lever following a sinusoidal trajectory.

B. Mechanical setup

We developed a custom-made mechanical setup in order to assess the performance of these ropes in walking-like conditions. This setup consists in a test bench driving a lever arm through cyclical movements (Fig. 3). A 220W brushless DC motor (DB87S01, Nanotec, Feldkirchen, Germany) actuates the bench, and is controlled by an open-source Vedder Electronic Speed Controller (VESC). The transmission system combines a 40:1 gearbox (PEII090-040, Apex Dynamics, Helmond, the Netherlands) and a 2:1 belt drive. The bench is equipped with a hall effect position sensor AS5048 and a custom force sensor using strain gages, that is placed on the level of the bench. The center of rotation of the bench lever is concentric with the one of the prosthesis joint, such as measuring the torque at this location is equivalent to measuring the prosthesis torque.

The lever arm of the bench is connected to a slider stretching the elastic element with a force F_{BE} (Fig. 4), with the bench simulating the movement of a user's body. The force F_{EB} from Fig. 2 is indeed the reaction force to F_{BE}, with the same magnitude but opposite direction.

At the other side of the rope, a mechanism is used to tune its pretension, with three different levels. A mechanical stop blocks the slider unidirectionally such that the rope can be pretensioned before running the loading cycles.

TABLE I. Specifications of the three ropes.

Rope Label	PE	PA1	PA2
Manufacturer Reference	Kanirope 13072	SWS B014C54EXW	Kanirope 10945
Material	Polyester	Polyamide	Polyamide
Diameter (mm)	3	3	3
Number of strands	8	16	8
Breaking strength (kN)	1.5	1.5	1.55
Elongation at break (%)	15-20	16 - 27	16 - 27

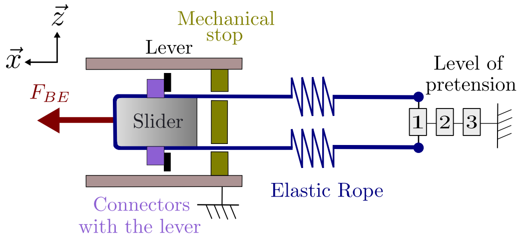

Fig. 4. Top view of the experimental setup: the rope is attached to a slider and is stretched with a variable pretension level, from 1 the least to 3 the most taut. During the stance phase, the test bench applies an axial force F_{BE} on the slider, stretching the elastic rope.

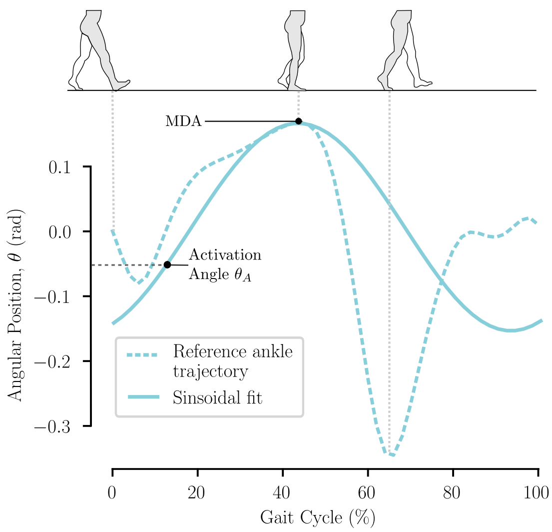

Fig. 5. The rope deformation is driven by a sinusoidal trajectory having the same amplitude as a sound ankle trajectory during the stance phase [19]. In particular, the same maximum dorsiflexion angle (MDA) is reached. The activation angle θ_A is the angle where the rope starts to be stretched, thus producing a reaction force F_{EB}.

C. Experimental Protocol

Typical ankle angular trajectory has been simplified as an equivalent sinusoidal trajectory displaying a similar amplitude and duration, i.e. as $\theta_{ref}(t) = A \sin(2\pi f t) + A_0$, with $A = 0.16\,rad$ and $A_0 = 0.01\,rad$. Three distinct levels of pretension can be tested, with level 1 corresponding to the neutral state of the rope. Levels 2 and 3 correspond to a rope pretension of about 2 and $4\,mm$, respectively, corresponding to pretension forces of about 25 % and 50 % of the target peak force. Two different frequencies are tested, i.e. $f = 0.2\,Hz$ and $1\,Hz$, capturing respectively very slow and fast walking. In particular, three experiments are conducted in order to assess the ropes performance under different conditions. Each time, a series of ten sinusoidal cyclical loadings is generated by the bench.

- Experiment 1: Loading the three different ropes with the highest level of pretension (level 3). This setting enables generating the highest force and thus assessing if the ropes can deliver enough force given the specifications. This is conducted with the bench moving at a slow frequency, i.e. $0.2\,Hz$.
- Experiment 2: Loading the rope PE with the three different levels of pretension. The aim is to quantify how this level of pretension influences the rope stiffness and force profile. This was performed again with a frequency of $0.2\,Hz$.
- Experiment 3: Loading the rope PE with different cycling frequencies. In particular, we compare the slow frequency ($0.2\,Hz$) with a frequency that is more consistent with a walking pace ($1\,Hz$). This aims at characterizing the visco-elastic behavior of the rope, i.e. potential speed-dependent effects on its efficiency. The second level of pretension is used for this experiment.

Experiments 2 and 3 are only reported for rope PE. However, unpublished data reveal similar results for both other ropes. Table II summaries the experimental conditions for each of the three experiments.

D. Equivalent Stiffness and Energy Efficiency

The rope stiffness is estimated for each experimental condition. It is taken as the best linear fit of the force-position curve during the linear region of the stretching phase. Given the configuration of the setup, this estimated stiffness is equivalent to twice the natural stiffness of the rope material.

The energy lost during the release phase is captured by the area inside the force-position plot. It corresponds to potential energy that is stored in the rope during the stretching phase and dissipated by friction during the release phase. It is computed as the time-integral of the mechanical power P_m:

$$\begin{aligned} E &= \int P_m(t)\,\mathrm{d}t = \int F_{EB}(t)\,\dot{x_e}(t)\,\mathrm{d}t \\ &= \int F_{EB}(x_e)\,\mathrm{d}x_e, \qquad (J) \end{aligned} \tag{5}$$

with $\dot{x_e}$ the linear speed at the extremity of the elastic element. The efficiency η can be expressed as the percentage of E_r – the energy released during the relaxing phase – over E_s – the energy stored in the rope during the stretching phase: $\eta = \frac{E_r}{E_s} \times 100, \ (\%)$. The efficiency η is equal to 100 % when all the energy stored in the elastic element is released.

IV. RESULTS & DISCUSSION

A. Experiment 1: Largest achievable force.

Fig. 6 depicts the force vs. position curve for each of the three tested ropes. Before the activation point x_A, i.e. about $-2\,mm$, the resulting force is zero. Then, the rope starts to stretch and energy is stored until the maximal position of $7.6\,mm$ is reached. After, the energy is released until the bench returns to the starting point. The stiffness of the ropes is highlighted by red dotted lines corresponding to the linear fit of the slope. Moreover, ripples are visible on the curves before and after the loading (leftmost sections of the curve. We speculate that this is due to non-linear dynamic

TABLE II. Conditions tested in the three experiments. The underlined parameter is the one particularly investigated.

Experiment ID	1	2	3
Rope type	<u>PE-PA1-PA2</u>	PE	PE
Pretension level	3	<u>1-2-3</u>	2
Actuation frequency	Slow	Slow	<u>Slow - Fast</u>

TABLE III. Efficiency and stiffness of the ropes in Experiments 1, 2 and 3 (mean ± std)

	Exp. 1: Rope label			**Exp. 2: Pretention level**			**Exp. 3: Frequency**	
	PE	PA1	PA2	1	2	3	Slow	Fast
Linear Stiffness, k_x (kN/mm)	0.14 ± 0.00	0.07 ± 0.00	0.10 ± 0.00	0.12 ± 0.00	0.13 ± 0.00	0.14 ± 0.00	0.14 ± 0.00	0.13 ± 0.02
Efficiency, η (%)	49.03 ± 0.25	51.65 ± 1.44	49.96 ± 0.81	44.81 ± 1.48	45.22 ± 0.79	49.03 ± 0.25	47.06 ± 0.83	47.88 ± 1.38

effects in the system's driving parts, such as an unbalance in the slider's guiding shaft. Further investigation is required to confirm this hypothesis.

Results are gathered in Table III. Specifications established that the target stiffness is about $0.15\,kN/mm$ for a $75\,kg$ user. Rope PE has a similar computed stiffness. It is thus a good candidate for this ankle prosthesis application. Ropes PA1 and PA2 have lower stiffness. Therefore, the force generated at maximum dorsiflexion is not high enough. They could however be more appropriate for users with a lower body weight. Energy efficiency has similar values for the three ropes, and this corresponds to important losses. In the best case (PA1), 48% of the elastic energy stored into the rope is lost, due to friction between the rope strands.

A good reproducibility over the cycles is observed in our experiments: standard deviation for the stiffness is lower than $1\,\%$ of the mean, while it is about $2\,\%$ for the energy efficiency. There is a good overlap of the force-position curves between the cycles, confirming that the three ropes stay within elastic regime, with no plastic deformations.

To sum up, the PE rope meets the specifications for a parallel elastic element in an ankle prosthesis regarding stiffness. However, energy losses are too high, leading to poor efficiency.

B. Experiment 2: Changing the level of pretension.

Three levels of pretension were tested on rope PE, see Fig. 7. By increasing this level of pretension, the rope is tauter before being engaged by the lever and thus the maximal achievable force is higher for the same displacement. This maximal force goes from $1.02\,kN$ (lowest pretention) to $1.49\,kN$ (highest pretension). Importantly, the rising phase of the tensioning phase does not display the same profile as a function of the level of pretention, i.e. for x_l between $-2\,mm$ and $0\,mm$. If pretension is not high enough (level 1), the rope is still slack when being elongated, and therefore the linear elastic regime is reached only after some elongation. In contrast, if the rope is too much pretensioned (level 3), there is first a large pretension force to be compensated before actually inducing some movement. This corresponds to a local stiffness that is higher at the beginning of the stretching phase. Level 2 represents a good compromise since local stiffness is quasi-linear at the beginning of the stretching phase.

Stiffness slightly increases with the level of pretension (Table III) although not to a large extend. Lower stiffness is likely due to non linear ramping-up profile at the beginning of the curve. Energy efficiency also increases with the level of pretension. This result is however marginal since all values stay below $50\,\%$.

C. Experiment 3: Changing the cycle frequency.

The force vs. position curve for the rope PE under two different loading frequencies is provided in Fig. 8. Both curves are overlapping, in particular in the stretching phase where stiffness was estimated. This leads to an estimated stiffness that is similar in both cases (Table III). Energy efficiency is also similar in both cases, i.e. around $47\,\%$. This tends to show that the viscoelastic behavior of the rope is dominated by dry friction phenomenon, which is not velocity-dependent.

V. CONCLUSION

In this paper, we investigated whether polymer-based ropes are good candidate for elastic energy storage in an ankle prosthesis application. Experiments were carried out on three ropes made of polyamide and polyester. The specifications for the required force and strain, and the corresponding constraints applied on the ropes, are based on typical dimensions of the target application, i.e. an ankle prosthesis.

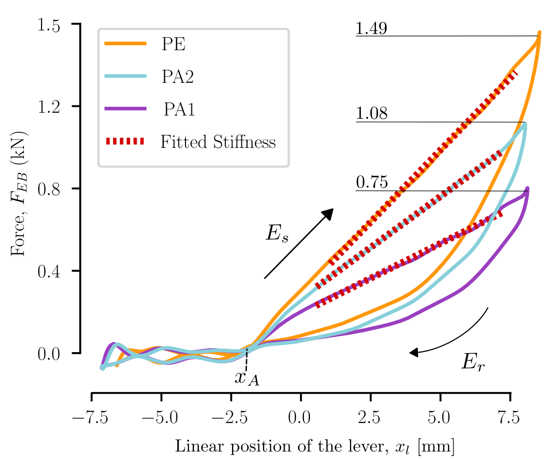

Fig. 6. Exp. 1: Force vs. linear position of the three ropes.

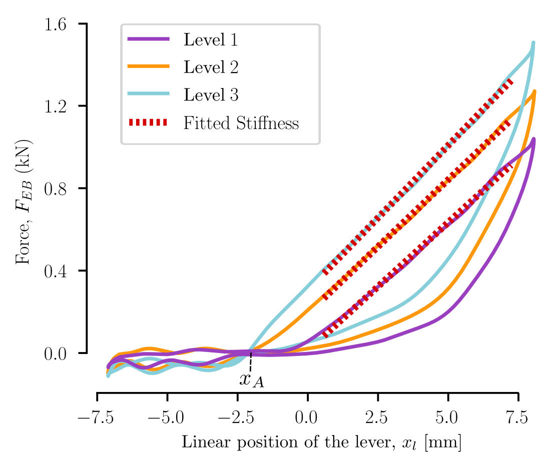

Fig. 7. Exp. 2: Force vs. position with rope PE. Three levels of pretension were tested, from the least taut (n°1) to the most taut (n°3).

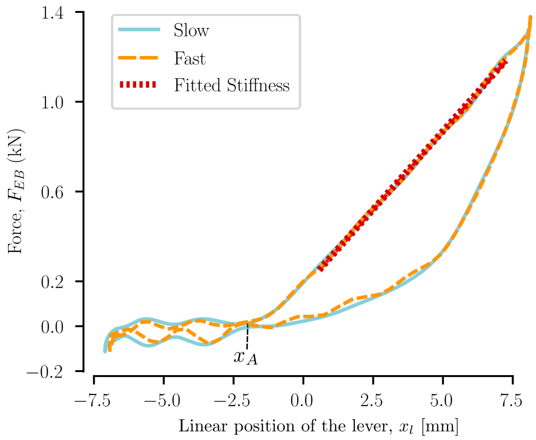

Fig. 8. Exp. 3: Force vs. position with rope PE at slow and fast speed.

Several conclusions can be drawn from these experiments. First, the rope stiffness mainly depends on the material and its configuration, such as the braiding and the number of strands. Polyester rope is stiffer than polyamide ones. We further observed that the pretension of the rope has to be tuned carefully. If the ropes are too stretched or not enough, the force profile is not linear in the early tensioning phase. Indeed, bump or slack are observed such that the stress-strain relationship reaches a linear elastic profile only after a certain level of tensioning. Increasing the level of pretension showed that we can increase by $150\,\%$ the achievable force. In the range of frequencies we tested, no effect is observed regarding neither the resulting stiffness nor the efficiency.

For the three experiments, the hysteresis in the force vs. position relationship is large. More precisely, only about $50\,\%$ of the elastic energy that is stored in the rope during the tensioning phase is released during the unstretching phase. The rest of this energy is lost in friction.

In conclusion, polymer-based artificial tendons fulfil several criteria for a typical application of ankle prosthesis. Because the ropes are light, compact, have a high yield strength, they could be good candidates for storing elastic energy and thus relaxing the requirements of the actuator. Nevertheless, the mechanical losses are significant, and further research should be conducted to improve their efficiency in returning the previously stored elastic energy.

REFERENCES

[1] Goodall, R and Hughes, W and Salciccioli, J and Marshall, D and Davies, AH and Shalhoub, J, "Trends in Lower Extremity Amputation Incidence in European Union 15+ Countries 1990-2017," *British Journal of Surgery*, vol. 108, 2021.

[2] Walter, Nike and Alt, Volker and Rupp, Markus, "Lower Limb Amputation Rates in Germany," *Medicina*, vol. 58, no. 1, pp. 101, 2022.

[3] Asif, Muhammad and Tiwana, Mohsin Islam and Khan, Umar Shahbaz and Qureshi, Waqar Shahid and Iqbal, Javaid and Rashid, Nasir and Naseer, Noman, "Advancements, Trends and Future Prospects of Lower Limb Prosthesis," *IEEE Access*, vol. 9, pp. 85956–85977, 2021.

[4] Russell Esposito, Elizabeth and Aldridge Whitehead, Jennifer M and Wilken, Jason M, "Step-to-step transition work during level and inclined walking using passive and powered ankle–foot prostheses," *Prosthetics and orthotics international*, vol. 40, no. 3, pp. 311–319, 2016.

[5] Klute, Glenn K and Kallfelz, Carol F and Czerniecki, Joseph M, "Mechanical properties of prosthetic limbs: adapting to the patient," *Journal of Rehabilitation Research & Development*, vol. 38, no. 3, 2001.

[6] Adamczyk, Peter Gabriel and Kuo, Arthur D, "Mechanisms of Gait Asymmetry Due to Push-Off Deficiency in Unilateral Amputees," *IEEE Transactions on Neural Systems and Rehabilitation Engineering*, vol. 23, no. 2, pp. 776–785, 2015.

[7] LeMoyne, Robert, "Advances for prosthetic technology," *Springer*, 2016.

[8] Gailey, Robert and Allen, Kerry and Castles, Julie and Kucharik, Jennifer and Roeder, Mariah, "Review of secondary physical conditions associated with lower-limb amputation and long-term prosthesis use," *Journal of Rehabilitation Research & Development*, vol. 45, no. 1, 2008.

[9] Struyf, Pieter A and van Heugten, Caroline M and Hitters, Minou W and Smeets, Rob J, "The prevalence of osteoarthritis of the intact hip and knee among traumatic leg amputees," *Archives of physical medicine and rehabilitation*, vol. 90, no. 3, pp. 440–446, 2009.

[10] Windrich, Michael and Grimmer, Martin and Christ, Oliver and Rinderknecht, Stephan and Beckerle, Philipp, "Active lower limb prosthetics: a systematic review of design issues and solutions," *Biomedical engineering online*, vol. 15, no. 3, pp. 5–19, 2016.

[11] Davidson, Audra M and Childers, W Lee and Chang, Young-Hui, "Altering the tuning parameter settings of a commercial powered prosthetic foot to increase power during push-off may not reduce collisional work in the intact limb during gait," *Prosthetics and Orthotics International*, vol. 45, no. 5, pp. 410–416, 2021.

[12] S. K. Au, P. Dilworth and H. Herr, "An ankle-foot emulation system for the study of human walking biomechanics," *Proceedings 2006 IEEE International Conference on Robotics and Automation*, pp. 2939–2945, 2006.

[13] Carney, Matthew E and Shu, Tony and Stolyarov, Roman and Duval, Jean-François and Herr, Hugh M, "Design and preliminary results of a reaction force series elastic actuator for bionic knee and ankle prostheses," *IEEE Transactions on Medical Robotics and Bionics*, vol. 3, no. 3, pp. 542–553, 2021.

[14] Tran, Minh and Gabert, Lukas and Hood, Sarah and Lenzi, Tommaso, "A lightweight robotic leg prosthesis replicating the biomechanics of the knee, ankle, and toe joint," *Science Robotics*, vol. 7, eabo3996, 2022.

[15] Jimenez-Fabian, Rene and Geeroms, Joost and Flynn, Louis and Vanderborght, Bram and Lefeber, Dirk, "Reduction of the torque requirements of an active ankle prosthesis using a parallel spring," *Robotics and Autonomous Systems*, vol. 92, pp. 187–196, 2017.

[16] Grimmer, Martin and Eslamy, Mahdy and Gliech, Stefan and Seyfarth, André, "A comparison of parallel- and series elastic elements in an actuator for mimicking human ankle joint in walking and running," *2012 IEEE International Conference on Robotics and Automation*, pp. 2463–2470, 2012.

[17] Au, Samuel K and Herr, Hugh M, "Powered ankle-foot prosthesis," *IEEE Robotics & Automation Magazine*, vol. 15, no. 3, pp. 52–59, 2008.

[18] Heremans, François and Vijayakumar, Sethu and Bouri, Mohamed and Dehez, Bruno and Ronsse, Renaud, "Bio-inspired design and validation of the Efficient Lockable Spring Ankle (ELSA) prosthesis," *2019 IEEE 16th International Conference on Rehabilitation Robotics (ICORR). IEEE*, 2019.

[19] D. A. Winter, "Biomechanics and Motor Control of Human Movement," 2009.

[20] Heremans, François and Ronsse, Renaud, "Design of an energy efficient transfemoral prosthesis using lockable parallel springs and electrical energy transfer," *2017 International Conference on Rehabilitation Robotics (ICORR)*, pp. 1305–1312, 2017.

[21] Lecomte, Christophe and Ármannsdóttir, Anna Lára and Starker, Felix and Tryggvason, Heimir and Briem, Kristin and Brynjolfsson, Sigurdur, "Variable stiffness foot design and validation," *Journal of Biomechanics*, vol. 122, p.110440, 2021.

[22] Shepherd, Max K., and Elliott J. Rouse. "The VSPA foot: A quasi-passive ankle-foot prosthesis with continuously variable stiffness," IEEE Transactions on Neural Systems and Rehabilitation Engineering, vol. 25, no. 12, pp. 2375–2386, 2017.

[23] Barry Cordage, "Technical Properties of Synthetic Fibers," 2012. Available: https://www.barry.ca/hubfs/info/rt-technical-properties-of-synthetic-fibres-en.pdf.